for these complexes and suggest equivalences in their K_{Pt} force constants. A narrow range, $1.69 < K_{Pt} < 1.85$ mdyn/Å, of solutions is seen which allow for a common K_{Pt} force constant. The choice of K_{Pt} does not alter the conclusion (as provided in the text) of the relative binuclear Pt(II) and Pt(III) bond strengths. Plots of K_{Pt} vs. I_{PtX} for these complexes (not shown) gives a near intercept (±0.02 mdyn/Å) of the curves with $K_{Pt} = 1.7$ mdyn/Å and $I_{PtX} = 0.16$ mdyn/Å and provides a reasonable solution. Values for K_{PtX} of 1.65, 1.45, and 1.16 mdyn/Å are readily obtained as shown in Figure 6. The calculated asymmetric ν(Pt–X) are 304, 206, and 161 cm^{-1} as obtained by $((K_{PtX})^{1/2}/\mu)/2\pi c$ and compare with the IR observations (295, 195, and 118 cm^{-1}). The large difference in ν(Pt–I) is attributed to mixing from an asymmetric ring mode and is discussed in the text.

Registry No. $K_4[Pt_2(pop)_4]$, 82135-51-1; $K_4[Pt_2(pop)_4Cl_2]$, 85335-49-5; $K_4[Pt_2(pop)_4Br_2]$, 82135-55-5; $K_4[Pt_2(pop)_4I_2]$, 85335-50-8; $K_4[Pt_2(pop)_4CH_3I]$, 82135-52-2.

Synthesis, Structure, and ^{195}Pt NMR Studies of Binuclear Complexes of *cis*-Diammineplatinum(II) with Bridging α-Pyridonate Ligands

L. Steven Hollis and Stephen J. Lippard*[†]

Contribution from the Department of Chemistry, Columbia University, New York, New York 10027.
Received November 15, 1982

Abstract: With ^{195}Pt NMR spectroscopy, several products formed in the reaction of *cis*-$[Pt(NH_3)_2(H_2O)_2]^{2+}$ with α-pyridone (C_5H_4NHO) have been identified in solution at pH 4.2. These complexes, present in the aqueous solution from which the *cis*-diammineplatinum α-pyridone blue is ultimately obtained, include $[Pt(NH_3)_2(OH)]_2^{2+}$, $[Pt(NH_3)_2(OH)]_3^{3+}$, *cis*-$[Pt(NH_3)_2(C_5H_4NOH)(H_2O)]^{2+}$, *cis*-$[Pt(NH_3)_2(C_5H_4NOH)_2]^{2+}$, and the head-to-head and head-to-tail α-pyridonate-bridged dimers $[Pt_2(NH_3)_4(C_5H_4NO)_2]^{2+}$. Crystals of the last two complexes were obtained from the reaction by careful control of the pH. A rational synthesis of the head-to-tail isomer was achieved from dimerization of *cis*-$[Pt(NH_3)_2(C_5H_4NOH)(H_2O)](NO_3)_2$. X-ray diffraction studies revealed the structure of the head-to-tail dimer, $[Pt_2(NH_3)_4(C_5H_4NO)_2](NO_3)_2\cdot 2H_2O$, to contain two α-pyridonate ligands bridging two *cis*-diammineplatinum(II) units with a Pt–Pt distance of 2.898 (1) Å. The head-to-head platinum(II) isomer dimerizes with itself in the crystal lattice to form a tetramer, $[Pt_2(NH_3)_4(C_5H_4NO)_2]_2(NO_3)_4$, that is held together by bridging α-pyridonate ligands and by stacking and intercation hydrogen-bonding interactions. The structure of this yellow complex is strikingly similar to that of the α-pyridone blue except for longer Pt–Pt distances, 2.877 (1) and 3.129 (1) Å vs. respective values of 2.775 (1) and 2.877 (1) Å in the blue, owing to differences in metal–metal bond order for the two complexes.

During the past decade the scope of aqueous platinum(II) chemistry has undergone a significant expansion with the discovery and exploration of the antitumor properties of *cis*-diamminedichloroplatinum(II), *cis*-DDP.[1] The growth in this area is presently being maintained by the widespread success that *cis*-DDP is finding in the clinical treatment of human cancer.[1c] One of the directives of work in this area continues to be the development of an understanding of the mechanism of drug action. Since the antitumor activity of *cis*-DDP is thought to result from the inhibition of cellular replication, induced by the interaction of the drug with DNA,[2] the study of the reactions of *cis*-DDP with nucleic acids and their constituents has become an active area of investigation.[3]

The chemistry of platinum–nucleotide interactions is a complex and diversified field of study. The reaction of *cis*-DDP or the aquated form of the complex, *cis*-$[Pt(NH_3)_2(H_2O)_2]^{2+}$, with free or substituted pyrimidine bases, leads to a variety of products[3-15] that can be classified according to the number of platinum atoms contained in the product molecule. A multiformity of simple mononuclear and binuclear platinum complexes of free and substituted uracil, thymine, and cytosine has been isolated and studied by ^{1}H NMR, vibrational spectroscopy, and X-ray crystallography.[5-15] In these compounds the platinum binds either, in mononuclear complexes, to one of the heterocyclic nitrogens (N1, N3) of the pyrimidine base or, in pyrimidine-bridged bi-

---

[†] Address correspondence to this author at the Department of Chemistry, Massachusetts Institute of Technology, Cambridge, MA 02139.

(1) (a) Rosenberg, B.; Van Camp, L. *Cancer Res.* **1970**, *30*, 1799. (b) Paoletti, C., Ed. *Biochemie* **1978**, *60*, 915–965. (c) Prestayko, A. E.; Crooke, S. T.; Carter, S. K., Eds. "Cisplatin, Status and New Developments"; Academic Press: New York, 1980. (d) Lippard, S. J. *Science (Washington, D.C.)* **1982**, *218*, 1075–1082.

(2) Roberts, J. J.; Thompson, A. J. *Prog. Nucleic Acid Res. Mol. Biol.* **1979**, *22*, 71.

(3) For a review see: Barton, J. K.; Lippard, S. J. In "Nucleic Acid–Metal Ion Interactions"; Spiro, T. G., Ed.; Wiley: New York, 1980; p 32.

(4) (a) Davidson, J. P.; Faber, P. J.; Fischer, R. G., Jr.; Mansy, S.; Peresie, H. J.; Rosenberg, B.; Van Camp, L. *Cancer Chemother. Rep.* **1975**, *59*, 287. (b) Lippert, B. *J. Clin. Hematol. Oncol.* **1977**, *7*, 26.

(5) (a) Lippert, B.; Pfab, R.; Neugebauer, D. *Inorg. Chim. Acta* **1979**, *37*, L495. (b) Lippert, B. *Ibid.* **1981**, *55*, 5. (c) Lippert, B. *Ibid.* **1981**, *56*, L23. (d) Lippert, B.; Neugebauer, D. *Ibid.* **1981**, *46*, 171. (e) Lippert, B.; Schubert, U. *Ibid.* **1981**, *56*, 15. (f) Lippert, B.; Neugebauer, D. *Inorg. Chem.* **1982**, *21*, 451. (g) Pfab, R.; Jandik, P.; Lippert, B. *Inorg. Chim. Acta* **1982**, *66*, 193.

(6) Lock, C. J. L.; Peresie, H. J.; Rosenberg, B.; Turner, G. *J. Am. Chem. Soc.* **1978**, *100*, 3371.

(7) Wu, S.-M.; Bau, R. *Biochem. Biophys. Res. Commun.* **1979**, *88*, 1435.

(8) (a) Lippert, B.; Lock, C. J. L.; Speranzini, R. A. *Inorg. Chem.* **1981**, *20*, 808. (b) Faggiani, R.; Lippert, B.; Lock, C. J. L. *Ibid.* **1982**, *21*, 3210.

(9) Faggiani, R.; Lippert, B.; Lock, C. J. L.; Pfab, R. *Inorg. Chem.* **1981**, *20*, 2381.

(10) Lippert, B.; Lock, C. J. L.; Speranzini, R. A. *Inorg. Chem.* **1981**, *20*, 335.

(11) Faggiani, R.; Lippert, B.; Lock, C. J. L. *Inorg. Chem.* **1980**, *19*, 295.

0002-7863/83/1505-3494$01.50/0 © 1983 American Chemical Society

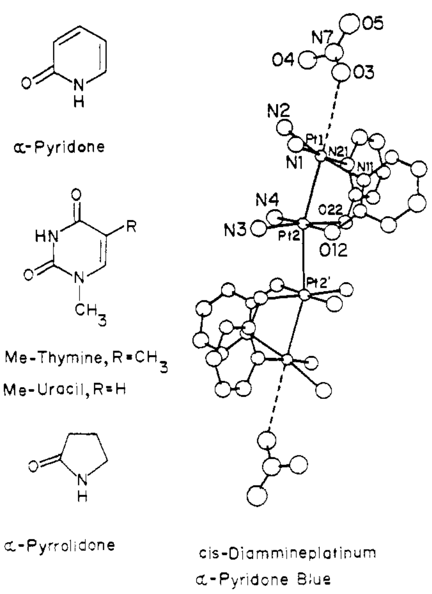

Figure 1. Structures of (left) α-pyridone and related cyclic amide ligands, which also form multinuclear complexes of *cis*-diammineplatinum, and (right) *cis*-diammineplatinum α-pyridone blue.

nuclear complexes, to a combination of N1 or N3 and one of the exocyclic atoms (O2, O4, N4). On the other hand, polynuclear species that are produced in many of the reactions of platinum with pyrimidines have been far more difficult to characterize structurally.[3-5] As recently suggested,[15] the difficulty in the isolation and characterization of the higher order condensation products results from the multiplicity and interconversion of the binding sites of both reactants. For example, in the reaction of *cis*-$[Pt(NH_3)_2(H_2O)_2]^{2+}$ with uracil, where there are four possible binding sites on the uracil ligand and two on the platinum atom, a variety of species have been detected in the ^1H NMR spectrum of the product.[15] Two additional features impede the characterization of many of the reaction components. They are ligand-exchange reactions, which interconvert the various products, and valence instability, which leads to the formation of partially oxidized materials, collectively known as the "platinum pyrimidine blues".[3]

One approach to this problem is to reduce product variability by limiting the number of binding sites available to platinum. This objective can be accomplished in two ways: the binding sites can be restricted by alkylating one of the heterocyclic nitrogens of the pyrimidine base, or the ligand can be replaced with a simplified base that retains the chemical and structural features of a pyrimidine. While both approaches have been used successfully, the latter method has been particularly useful in modeling the formation of the blue species that results from the partial oxidation of amidate-bridged oligomers.[16] Indeed, much of our understanding of the platinum pyrimidine blues is based on the study of the reaction of *cis*-$[Pt(NH_3)_2(H_2O)_2]^{2+}$ with the pyrimidine analogue α-pyridone, from which the first crystalline platinum blue was isolated.[16-18]

The reaction of *cis*-$[Pt(NH_3)_2(H_2O)_2]^{2+}$ with α-pyridone, under conditions identical with those used in the preparation of the pyrimidine blues, produces darkly colored solutions that, upon addition of nitric acid, yield dark blue crystals of *cis*-diammineplatinum α-pyridone blue, $[(NH_3)_2Pt(C_5H_4NO)_2Pt(NH_3)_2]_2(NO_3)_5{\cdot}H_2O$ (PPB).[17] Crystallographic studies have shown the structure of PPB to consist of a tetranuclear chain of *cis*-diammineplatinum units that is composed of two dimeric fragments, bridged in a head-to-head fashion by α-pyridonate ligands (Figure 1). As demonstrated by ESR,[17b] XPS,[19] and optical studies,[20] the platinum chain of PPB, formally comprised of three Pt(II) and one Pt(III) centers, contains one unpaired electron delocalized over the length of the chain in a molecular orbital having metal-metal σ^* character. It has been shown,[16-18] from a comparative study of spectroscopic, magnetic, and chemical properties, that the pyrimidine blues also contain partially oxidized, multinuclear chains of amidate bridged *cis*-diammineplatinum units. The difference between the α-pyridone and pyrimidine blues derives from the variability in the mode of attachment of the pyrimidine ligand which produces oligomers of varying chain length.[16] While a comparison of the properties of PPB and the pyrimidine blues has revealed much about the nature of platinum blues, a similar comparison of the nonblue (Pt(II)) products that are formed during and prior to the formation of the blues has not been conducted.

The present study examines the reactions that lead to the formation of PPB and compares the nonblue α-pyridone reaction products with those of the pyrimidines. As a follow-up to our preliminary work,[21] we report here the preparation and structural details of two of the major components of these reactions: the head-to-tail and head-to-head isomers of the bis(μ-pyridonato) dimers of *cis*-diammineplatinum(II). We also present the results of ^{195}Pt NMR experiments that reveal the nature of the products of the reaction of *cis*-$[Pt(NH_3)_2(H_2O)_2]^{2+}$ with α-pyridone in solution. This information has led to a unified picture of the chemistry that precedes and accompanies the formation of the *cis*-diammineplatinum α-pyridone blue.

Experimental Section

Preparation of Compounds. All platinum complexes were prepared from *cis*-$[Pt(NH_3)_2Cl_2]$ which was obtained, via the method of Dhara,[22] from $K_2[PtCl_4]$ (Engelhard). α-Pyridone (Aldrich Chemical Co.) was purified by recrystallization from benzene. All other reagents were obtained from commercial sources. Elemental analyses were performed by Galbraith Laboratories, Knoxville, TN.

Bis(μ-2-pyridonato-*N*1,*O*2)bis(*cis*-diammineplatinum(II)) Dinitrate Dihydrate, $[Pt_2(NH_3)_4(C_5H_4NO)_2](NO_3)_2{\cdot}2H_2O$ (1): Head-to-Tail Isomer. Method 1. This compound can be isolated directly from the α-pyridone blue reaction[17] as follows. An aqueous solution of *cis*-$[Pt(NH_3)_2(NO_3)_2]$[23] (1 mmol/6 mL) and α-pyridone (1 mmol) was adjusted to pH 6.0 and allowed to react for 1 day at 40 °C. The pH of the resulting dark green solution (pH 4.2) was adjusted to 1.0 with concentrated HNO_3 and placed in an ice bath (0 °C) for 3 h. The crystals that formed during this period were collected by filtration, and the volume of the filtrate was reduced by air evaporation. The crystalline material was found to be a mixture of two products: blue needles (PPB) and light green blocks (compound **1**). A second crop of crystals, which contained a greater proportion of **1**, was obtained from cooling the filtrate after 1-2 days of air evaporation. Pure, pale yellow samples of **1** were obtained from this material by fractional crystallization from water; typical yields were 100 mg of **1** (25%). Anal. Calcd for $Pt_2C_{10}H_{24}N_8O_{10}$ (**1**): C, 14.89; H, 3.00; N, 13.89. Found: C, 14.85; H, 3.06; N, 13.83. ^1H NMR (Me_2SO-d_6) δ 8.10 (d, Pt satellites, H_6), 7.24 (t, H_4), 6.42 (t, H_3, H_5), 4.54-4.39 (br, overlapping peaks, Pt satellites, NH_3); UV-visible spectrum of **1** (water) λ 298 nm (ϵ 5300 cm^{-1} M^{-1}), 220 (sh, ϵ ~36 000 cm^{-1} M^{-1}).

Method 2. The head-to-tail dimer **1** was also prepared from the dimerization reaction of the aquo α-pyridone complex *cis*-$[Pt(NH_3)_2(C_5H_4NOH)(H_2O)](NO_3)_2$. An aqueous solution (~0.1 M) of 150 mg of *cis*-$[Pt(NH_3)_2(C_5H_4NOH)Cl]Cl$ (see below) was stirred with 2 equiv of $AgNO_3$ for 24 h in the dark, and AgCl was then removed by filtration after cooling to 0 °C for 2 h. This solution (pH 2) was adjusted to pH

---

(12) Faggiani, R.; Lock, C. J. L.; Pollock, R. J.; Rosenberg, B.; Turner, G. *Inorg. Chem.* **1981**, *20*, 804.

(13) Faggiani, R.; Lippert, B.; Lock, C. J. L.; Speranzini, R. A. *J. Am. Chem. Soc.* **1981**, *103*, 1111.

(14) Lippert, B.; Neugebauer, D.; Schubert, U. *Inorg. Chim. Acta* **1980**, *46*, L11.

(15) Lippert, B. *Inorg. Chem.* **1981**, *20*, 4326.

(16) Barton, J. K.; Lippard, S. J. *Ann. N.Y. Acad. Sci.* **1978**, *313*, 686.

(17) (a) Barton, J. K.; Rabinowitz, H. N.; Szalda, D. J.; Lippard, S. J. *J. Am. Chem. Soc.* **1977**, *99*, 2827. (b) Barton, J. K.; Szalda, D. J.; Rabinowitz, H. N.; Waszczak, J. V.; Lippard, S. J. *Ibid.* **1979**, *101*, 1434.

(18) Barton, J. K.; Caravana, C.; Lippard, S. J. *J. Am. Chem. Soc.* **1979**, *101*, 7269.

(19) Barton, J. K.; Best, S. A.; Lippard, S. J.; Walton, R. A. *J. Am. Chem. Soc.* **1978**, *100*, 3785.

(20) Fanwick, P. E.; Hollis, L. S.; Lippard, S. J., to be submitted for publication.

(21) Hollis, L. S.; Lippard, S. J. *J. Am. Chem. Soc.* **1981**, *103*, 1230.

(22) Dhara, S. G. *Indian J. Chem.* **1970**, *8*, 193.

(23) Lippert, B.; Lock, C. J. L.; Rosenberg, B.; Zvagulis, M. *Inorg. Chem.* **1977**, *16*, 1525.

6.5 with 1 N NaOH, and the resulting solution was allowed to stand for 1.5 days at room temperature (~24 °C). After cooling the solution to 0 °C for 4 h, crystals of **1** were collected and washed with water. A second crop of crystals was obtained by air evaporation of the filtrate. The combined yield was 80 mg (52%).

Method 3. Compound **1** was also obtained from the reaction of *cis*-$[Pt(NH_3)_2(NO_3)_2]$ with α-pyridone as described in method 1 but with one modification: the pH of the solution was not adjusted after incubation at 40 °C. This solution was evaporated for 2 days in air and cooled to 0 °C for 2 h. The resulting grey-brown precipitate was collected by filtration, and **1** was isolated in 15–20% yields from this material by fractional crystallization from water.

Bis(μ-2-pyridonato-*N*1,*O*2)bis(*cis*-diammineplatinum(II)) Dinitrate, $[Pt_2(NH_3)_4(C_5H_4NO)_2]_2(NO_3)_4$ (2): Head-to-Head Isomer. Method 1. Compound **2** was obtained from the reaction described in method 3 of the preparation of the head-to-tail dimer **1**. The brown-grey precipitate from the reaction was crystallized two times from water, and the filtrates were concentrated with a rotoevaporator and cooled to 0 °C for 1 h. Dark green crystals of compound **2** were collected by filtration and washed with water (yield 10%). Recrystallization of the dark crystals from water produced yellow crystals of **2**. The dark color was found to be surface contamination that results from crystal growth in the dark green filtrate of the crude product. Anal. Calcd for $Pt_2C_{10}H_{20}N_8O_8$ (**2**): C, 15.59; H, 2.62; N, 14.54. Found: C, 15.42; H, 2.57; N, 14.46. ^1H NMR (Me_2SO-d_6) δ 8.18 (d, Pt satellites, H_6), 7.33 (t, H_4), 6.51 (t, H_3, H_5), 4.55 (br, overlapping peaks, Pt satellites, NH_3).

Method 2. The head-to-head complex **2** was also obtained by adding a solution containing 0.1 mmol of $[Pt_2(NH_3)_4(OH)_2](NO_3)_2$[24] dissolved in 8 mL of water to 0.1 mmol of α-pyridone in 1 mL of water, adjusting the pH to 10 with 1 N NaOH, and warming the solution to 37 °C for 24 h (final pH 7.5). Air evaporation of the resulting solution provided the following products: the dihydroxo-bridged starting material (~80% yield), the head-to-tail dimer **1** (~10% yield), and **2** (5% yield). Crystals of **2** were separated from the sample with a dissecting needle under a microscope. The product identity was confirmed from the crystallographic unit cell parameters.

***cis*-Chloro(2-hydroxypyridine)diammineplatinum(II) Chloride, *cis*-$[Pt(NH_3)_2(C_5H_4NOH)Cl]Cl$ (3). Method 1.** Compound **3** was obtained by heating 6.67 mmol of *cis*-$[Pt(NH_3)_2Cl_2]$ and 15 mmol of α-pyridone in 180 mL of water to 65 °C for 48 h with stirring. The volume of the resulting amber solution was reduced with a rotoevaporator to 15 mL, cooled to 0 °C for 1.5 h, and filtered to remove unreacted starting material (0.5 g of *cis*-$[Pt(NH_3)_2Cl_2]$). Continued evaporation followed by the addition of chloroform produced a light biege product, which was filtered and air dried (1.7 g). Recrystallization of this material from isopropanol/0.1 N HCl gave 0.85 g of **3** as white needles (32% yield). Anal. Calcd for $PtC_5H_{11}N_3OCl_2$ (**3**): C, 15.20; H, 2.81; N, 10.63; Cl, 17.94. Found: C, 15.15; H, 2.72; N, 10.57; Cl, 17.72. ^1H NMR (D_2O, pH 1 with DCl) δ 8.35 (t, H_6, Pt satellites), 7.84 (t, H_4), 7.03 (m, H_3, H_5), 4.15 (br, overlapping peaks, NH_3); UV–visible spectrum of **3** (water; pH 2, with 1 N HCl) λ 278 nm (ε 5000 cm^{-1} M^{-1}), 248 (sh, ε ~1800 cm^{-1} M^{-1}).

Method 2. Compound **3** was also obtained from the reaction of α-pyridone with *cis*-$[Pt(NH_3)_2Cl_2]$ (14.6 mmol) by reaction with 1 equiv of $AgNO_3$ in 130 mL of water for 2 h at 50 °C. After an additional 20 h of stirring at room temperature the AgCl was removed by filtration, and the yellow filtrate was warmed to 55 °C for 1.5 h following the addition of 1.1 equiv of α-pyridone. The volume of the solution was then reduced to 25 mL with a rotoevaporator (50 °C), and the resulting yellow precipitate (*cis*-$[Pt(NH_3)_2Cl_2]$) was removed by filtration. The green filtrate was treated with concentrated HCl to discharge the green color (pH 1) and placed on ice. A cream-colored precipitate, which contains a mixture of the NO_3^- and Cl^- salts of *cis*-$[Pt(NH_3)_2(C_5H_4NOH)Cl]^+$, was collected by filtration after 2 h at 0 °C. White needles of **3** were obtained by recrystallization of this material from 1 N HCl/isopropanol: yield 1.4 g (24%).

Spectral Measurements. Proton NMR spectra were recorded with a Bruker WP-80 spectrometer, and all chemical shifts were measured relative to DSS. Natural abundance ^{195}Pt NMR spectra were obtained on a Bruker WM-300 spectrometer with a wide-bore (20 mm) Pt probe at 64.5 MHz. Spectral data were acquired with a 6-μs pulse (~6° tilt angle) and a 6-μs acquisition time, with a spectral width of either 83 or 100 kHz, collected in 8K data points. Chemical shifts were measured relative to 0.2 M K_2PtCl_4 (in 0.4 M KCl/D_2O), which was used as an internal reference (−1627.0 ppm vs. 0.2 M K_2PtCl_6 in H_2O) in a 5-mm concentric tube insert. Sample temperature was regulated at 25 °C by using the Bruker variable-temperature controller. UV–visible spectra were obtained with a Cary 118 C spectrophotometer.

Collection and Reduction of X-ray Data. $[Pt_2(NH_3)_4(C_5H_4NO)_2](NO_3)_2 \cdot 2H_2O$ (1), Head-to-Tail Dimer. The pale yellow crystal used in the diffraction study was a parallelepiped with dimensions of 0.20 mm × 0.12 mm × 0.07 mm bounded by the faces (100), $(\bar{1}00)$, $(\bar{1}11)$, $(1\bar{1}\bar{1})$, $(\bar{1}\bar{1}1)$, and $(11\bar{1})$. The quality of the crystal was examined by taking open counter ω scans of several low-angle reflections and was found to be acceptable ($\Delta\bar{\omega}_{1/2} \sim 0.08°$). The intensity data and unit cell parameters were measured with a single-crystal diffractometer as described in Table I.[26] The space group was determined to be either $C2/c$ (C_{2h}^6, No. 15) or Cc (C_s^4, No. 9)[27] from the systematic absences hkl, $h + k = 2n + 1$, and $h0l$, $l = 2n + 1$, and the former choice was confirmed by the successful solution and refinement of the structure.

$[Pt_2(NH_3)_4(C_5H_4NO)_2](NO_3)_4$ (2), Head-to-Head Isomer. The yellow crystal that was used for data collection was irregular in shape with dimensions of 0.23 mm × 0.13 mm × 0.08 mm and was bounded by the faces (101), $(\bar{1}0\bar{1})$, $(01\bar{1})$, $(0\bar{1}1)$, $(\bar{1}10)$, $(1\bar{1}0)$, and $(\bar{1}11)$. Inspection of several low-angle ω scans indicated the crystal to be acceptable for data collection ($\Delta\bar{\omega}_{1/2} = 0.08°$). The space group was determined to be $P2_1/n$ (C_{2h}^5, No. 14, in a nonstandard setting)[28] from the systematic absences $h0l$, $h + l = 2n + 1$, and $0k0$, $k = 2n + 1$. Further details of the data collection and reduction are presented in Table I.

Structure Solution and Refinement. $[Pt_2(NH_3)_4(C_5H_4NO)_2](NO_3)_2 \cdot 2H_2O$ (1). The structure was solved in $C2/c$ by standard Patterson and Fourier methods and refined[29] by using anisotropic thermal parameters for all non-hydrogen atoms. Neutral atom scattering factors and anomalous dispersion corrections for non-hydrogen atoms were obtained from ref 30; hydrogen atom scattering factors were taken from ref 31. The positions of all hydrogen atoms were refined with constraints using isotropic thermal parameters. The hydrogen atoms of the α-pyridonate ring were placed at calculated positions (C–H = 0.95 Å) and constrained to "ride" on the carbon atoms to which they are attached.[29] The hydrogen atoms of the ammine ligands were refined as a rigid group by fixing[29] the following interatomic distances: N–H = 0.87 (1) Å; H–H = 1.42 (1) Å; Pt–H = 2.48 (1) Å, for each hydrogen in the group. The hydrogen atoms of the pyridonate ring and of each ammine ligand were each given an independent set of common thermal parameters in the refinement. The hydrogen atoms of the water molecules of hydration (O1) were not located.

Full-matrix least-squares refinement of the structure using 157 parameters converged at $R_1 = 0.032$ and $R_2 = 0.040$.[32] The function minimized during refinement was $\sum w(|F_o| - |F_c|)^2$, where $w = 1.000/[\sigma^2(F_o) + 0.000625F_o^2]$. The maximum ratio of parameter shift to estimated standard deviation in the final cycle of refinement was 0.1, and the largest peaks on the final difference map were ≤1.4 e A^{-3} and were in the vicinity of the Pt atom (≤1.4 Å). The average $w\Delta^2$ for groups of data sectioned according to parity group, $\sin \theta/\lambda$, $|F_o|$, $|h|$, $|k|$, or $|l|$, showed good consistency, and the weighting scheme was considered to be acceptable.

$[Pt_2(NH_3)_4(C_5H_4NO)_2]_2(NO_3)_4$ (2). The positions of the two unique Pt atoms were found from a Patterson map. Phasing of the data using these refined positions provided the locations of all non-hydrogen atoms in the difference Fourier map. As described above, all non-hydrogen atoms were refined with anisotropic thermal parameters, and hydrogen atoms were refined with constraints using common isotropic thermal parameters for each set of ammine and α-pyridonate ring hydrogens.

Full-matrix least-squares refinement of the structure using 295 variable parameters converged at $R_1 = 0.038$ and $R_2 = 0.045$.[32] The weighting function used in the refinement was $w = 0.9688/[\sigma^2(F_o) + 0.000625F_o^2]$, and the maximum parameter shift, found in the final cycle of refinement, was 0.2σ (H atom on N3). The only residual peaks of significant height (≤1.9 e A^{-3}) that were observed in the final difference Fourier map were found to lie within 1.1 Å from the platinum atoms. The $w\Delta^2$ values for groups of data sectioned as above showed good

---

(24) (a) Stanko, J. A.; Hollis, L. S.; Schreifels, J. A.; Hoeschele, J. D. *J. Clin. Hematol. Oncol.* **1977**, *7*, 138. (b) Faggiani, R.; Lippert, B.; Lock, C. J. L.; Rosenberg, B. *J. Am. Chem. Soc.* **1977**, *99*, 777.

(25) Churchill, M. R.; Kalra, K. L. *Inorg. Chem.* **1974**, *13*, 1427.

(26) Silverman, L. D.; Dewan, J. C.; Giandomenico, C. M.; Lippard, S. J. *Inorg. Chem.* **1980**, *19*, 3379.

(27) "International Tables for X-ray Crystallography", 3rd ed.; Kynoch Press: Birmingham, England, 1973; Vol I, pp 89, 101.

(28) Reference 27, p 99.

(29) All calculations were preformed on a DEC VAX-11/780 computer using SHELX-76: Sheldrick, G. M. In "Computing in Crystallography"; Schenk, H., Olthof-Hazekamp, R., van Koningsveld, H., Bassi, G. C., Eds.; Delft University Press: Delft, The Netherlands, 1978; pp 34–42.

(30) "International Tables for X-ray Crystallography"; Kynoch Press: Birmingham, England, 1974; Vol. IV, pp 99, 149.

(31) Stewart, R. F.; Davidson, E. R.; Simpson, W. T. *J. Chem. Phys.* **1965**, *42*, 3175.

(32) $R_1 = \sum||F_o| - |F_c||/\sum|F_o|$; $R_2 = [\sum w(|F_o| - |F_c|)^2/\sum w|F_o|^2]^{1/2}$.

Table I. Experimental Details of the X-ray Diffraction Studies of $[Pt_2(NH_3)_4(C_5H_4NO)_2](NO_3)_2·2H_2O$ (1) and $[Pt_2(NH_3)_4(C_5H_4NO)_2]_2(NO_3)_4$ (2)

(A) Crystal Parameters[a] at 23 °C

	1	2		1	2
a, Å	15.440 (4)	9.158 (1)	space group	*C*2/*c*	$P2_1/n$
b, Å	14.350 (2)	9.907 (1)	*Z*	4	4
c, Å	10.6674 (8)	21.405 (1)	ρ(calcd), g cm^{-3}	2.569	2.655
β, deg	118.09 (2)	96.979 (8)	ρ(obsd), g cm^{-3}	2.56 (2)[b]	2.67 (2)[b]
V, Å^3	2085.1	1927.6	mol wt	806.5	770.5

(B) Measurement of Intensity Data[c]

	1	2
instrument: Enraf-Nonius CAD-4F κ-geometry diffractometer		
radiation: Mo Kα ($\lambda_{\bar{\alpha}}$ = 0.710 73 Å) graphite monochromatized		
standards,[d] measd every 1 h of X-ray exposure time	$(2,\underline{0},0)$ $(\underline{4},\underline{6},4)$ $(5,\bar{1},2)$	$(2,\underline{1},\bar{4})$ $(1,\bar{1},\underline{1})$ $(1,3,\bar{3})$
no. of reflctns collected (non space group extinguished)	3122 [$3 \leqslant 2\theta \leqslant 55°$ ($\pm h, +k, +l$); $3 \leqslant 2\theta \leqslant 30°$ ($\pm h, -k, +l$)]	5087 [$3 \leqslant 2\theta \leqslant 55°$ ($\pm h, +k, +l$); $3 \leqslant 2\theta \leqslant 20°$ ($\pm h, -k, -l$)]

(C) Treatment of Intensity Data[e]

	1	2
μ, cm^{-1}	136.1	147.1
transmission factor range[f]	0.22-0.43	0.07-0.39
averaging, R_{av}[c]	0.064	0.056
no. of reflctns after averaging	2402	4417
obsd unique data	1864	2738
$F_o > n\sigma(F_o)$	$n = 4$	$n = 6$

[a] From a least-squares fit of the setting angles of 25 reflections with $2\theta > 30°$. [b] By flotation in a mixture of $CHBr_3$ and $CHCl_3$. [c] See ref 26 for typical data collection and reduction procedures employed in our laboratory. [d] Used to scale the data for anisotropic decay; ~4% for 1 and 3% for 2 (see ref 25). [e] F_o and $\sigma(F_o)$ were corrected for background, attenuator, and Lorentz-polarization of X-radiation as described previously (see ref 26). [f] Absorption corrections were performed with the Wehe-Busing-Levey ORABS program.

Table II. Final Positional Parameters for $[Pt_2(NH_3)_4(C_5H_4NO)_2](NO_3)_2·2H_2O$ (**1**)[a]

atom	*x*	*y*	*z*
Pt	0.43312 (2)	0.24116 (2)	0.59878 (3)
O2	0.3764 (3)	0.3489 (3)	0.6589 (5)
N1	0.5353 (4)	0.3289 (4)	0.5951 (6)
N2	0.3236 (4)	0.1580 (4)	0.5950 (7)
N3	0.4844 (6)	0.1350 (5)	0.5250 (8)
C6	0.5239 (6)	0.3527 (7)	0.4664 (9)
H6	0.4759 (6)	0.3214 (7)	0.3847 (9)
C5	0.5808 (6)	0.4222 (8)	0.4496 (10)
H5	0.5725 (6)	0.4372 (8)	0.3578 (10)
C4	0.6485 (6)	0.4685 (6)	0.5671 (11)
H4	0.6857 (6)	0.5180 (6)	0.5569 (11)
C3	0.6629 (6)	0.4435 (5)	0.6994 (9)
H3	0.7111 (6)	0.4741 (5)	0.7817 (9)
C2	0.6046 (5)	0.3710 (4)	0.7124 (8)
N4	0.3763 (5)	−0.0803 (5)	0.6565 (9)
O41	0.3961 (5)	−0.0245 (4)	0.7546 (6)
O42	0.3774 (6)	−0.1641 (5)	0.6786 (9)
O43	0.3552 (5)	−0.0499 (5)	0.5359 (7)
O1	0.2601 (6)	0.1927 (5)	0.8163 (8)
H1N2	0.341 (2)	0.0996 (6)	0.601 (6)
H2N2	0.2697 (13)	0.166 (3)	0.516 (3)
H3N2	0.313 (3)	0.172 (3)	0.666 (4)
H1N3	0.486 (4)	0.0834 (11)	0.569 (5)
H2N3	0.5434 (19)	0.148 (2)	0.538 (6)
H3N3	0.446 (3)	0.127 (3)	0.4340 (18)

[a] Atoms are labeled as shown in Figure 2. Estimated standard deviations in the last significant digit(s) are given in parentheses.

consistency, and the weighting function was found acceptable.

Results and Discussion

Description of the Structures. The final atomic positional parameters together with their estimated standard deviations are presented in Tables II and III. Interatomic distances and angles are reported in Tables IV and V. A listing of thermal parameters and a summary of observed and calculated structure factor amplitudes for **1** and **2** are available as supplementary material (Tables S1–S4). Figure 2 depicts the coordination geometry and atom labeling scheme for the head-to-tail isomer of the $[Pt_2(NH_3)_4(C_5H_4NO)_2]^{2+}$ cation; the structure of the head-to-head isomer is shown in Figure 3.

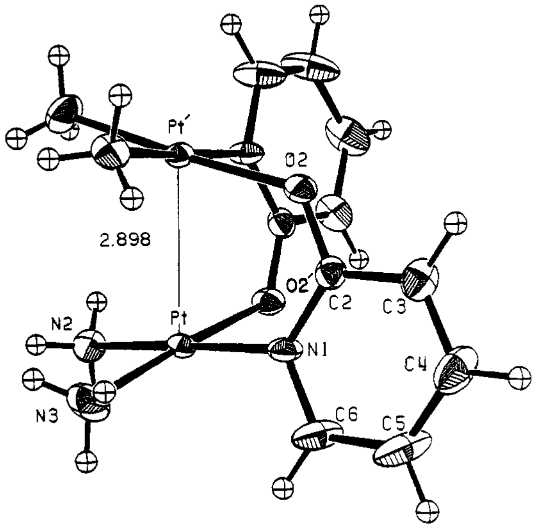

Figure 2. ORTEP illustration of the structure of the head-to-tail isomer of the α-pyridonate-bridged cation $[Pt_2(NH_3)_4(C_5H_4NO)_2]^{2+}$ (**1**), showing the 40% probability thermal ellipsoids and the Pt-Pt distance (angstroms). For clarity, the hydrogen atoms are depicted as spheres with *B* set to 1 Å^2. The cation is found to lie on a crystallographic 2-fold axis (perpendicular to the Pt-Pt′ vector) which relates the two halves of the dimer. The labels of the hydrogen atoms (not shown) are numbered according to the atom to which they are attached (H1N2 is attached to N2 and H6 to C6, etc.).

$[Pt_2(NH_3)_4(C_5H_4NO)_2](NO_3)_2·2H_2O$ (1), Head-to-Tail Dimer. The cation (Figure 2) lies on a crystallographic 2-fold axis, and there are equal amounts of both optical isomers in the centrosymmetric crystal lattice. The platinum coordination geometry is typical of square-planar Pt(II) complexes. The only feature

Table III. Final Positional Parameters for $[Pt_2(NH_3)_4(C_5H_4NO)_2]_2(NO_3)_4$ (2)[a]

atom	*x*	*y*	*z*
Pt1	0.08551 (5)	0.22279 (5)	−0.16796 (2)
Pt2	0.00184 (5)	0.05566 (5)	−0.06831 (2)
N2	−0.0855 (11)	0.1705 (11)	−0.2355 (5)
N1	0.2271 (12)	0.1022 (10)	−0.2106 (5)
N11	0.2570 (11)	0.2677 (10)	−0.1013 (5)
N21	−0.0448 (10)	0.3580 (10)	−0.1284 (5)
N3	0.0555 (13)	−0.1335 (10)	−0.0966 (5)
N4	−0.2191 (11)	0.0246 (12)	−0.0896 (6)
O12	0.2202 (9)	0.0803 (8)	−0.0393 (4)
O22	−0.0469 (10)	0.2407 (8)	−0.0358 (4)
C22	−0.0786 (13)	0.3486 (12)	−0.0700 (7)
C23	−0.1462 (14)	0.4588 (13)	−0.0418 (7)
H23	−0.1658 (14)	0.4534 (13)	0.0007 (7)
C24	−0.1827 (15)	0.5720 (14)	−0.0765 (7)
H24	−0.2296 (15)	0.6453 (14)	−0.0584 (7)
C25	−0.1516 (14)	0.5802 (13)	−0.1375 (7)
H25	−0.1760 (14)	0.6589 (13)	−0.1619 (7)
C26	−0.0840 (15)	0.4711 (12)	−0.1630 (6)
H26	−0.0644 (15)	0.4753 (12)	−0.2055 (6)
C12	0.2983 (12)	0.1820 (13)	−0.0538 (6)
C13	0.4353 (13)	0.2028 (15)	−0.0163 (7)
H13	0.4682 (13)	0.1401 (15)	0.0159 (7)
C14	0.5206 (16)	0.3125 (16)	−0.0263 (8)
H14	0.6129 (16)	0.3257 (16)	−0.0016 (8)
C15	0.4696 (16)	0.4047 (17)	−0.0734 (8)
H15	0.5229 (16)	0.4852 (17)	−0.0790 (8)
C16	0.3392 (14)	0.3767 (13)	−0.1121 (7)
H16	0.3079 (14)	0.4348 (13)	−0.1465 (7)
N7	0.0531 (13)	0.2000 (13)	0.2612 (6)
N8	0.0582 (17)	0.3066 (15)	−0.3606 (5)
O71	0.0945 (14)	0.2971 (13)	0.2964 (6)
O72	0.1461 (11)	0.1371 (10)	0.2351 (6)
O73	−0.0782 (12)	0.1734 (13)	0.2471 (6)
O81	−0.0710 (15)	0.3044 (15)	−0.3557 (7)
O82	0.1179 (16)	0.4015 (14)	−0.3818 (6)
O83	0.1260 (19)	0.1986 (15)	−0.3487 (7)
H1N1	0.179 (3)	0.034 (6)	−0.229 (4)
H2N1	0.296 (7)	0.072 (9)	−0.1825 (12)
H3N1	0.267 (9)	0.149 (3)	−0.239 (4)
H1N2	−0.111 (6)	0.087 (3)	−0.230 (2)
H2N2	−0.059 (3)	0.180 (7)	−0.2729 (5)
H3N2	−0.161 (3)	0.222 (5)	−0.232 (2)
H1N3	0.009 (9)	−0.151 (5)	−0.134 (2)
H2N3	0.031 (11)	−0.1941 (15)	−0.070 (3)
H3N3	0.150 (3)	−0.139 (4)	−0.099 (5)
H1N4	−0.2355 (17)	−0.058 (4)	−0.103 (5)
H2N4	−0.255 (3)	0.081 (8)	−0.119 (4)
H3N4	−0.263 (2)	0.036 (11)	−0.0561 (15)

[a] Atoms are labeled as shown in Figure 3. The atoms of the α-pyridonate rings are labeled according to their ring number followed by their ring position; for example, ring 1 contains N11, C12–C16, etc. Estimated standard deviations in the last significant digits(s) are given in parentheses.

Table IV. Interatomic Distances (Å) and Angles (deg) for $[Pt_2(NH_3)_4(C_5H_4NO)_2](NO_3)_2 \cdot 2H_2O$ (1)[a]

Coordination Sphere			
Pt-Pt′	2.8981 (5)	Pt-N3	2.038 (6)
Pt-N1	2.032 (6)	Pt-O2′	2.024 (5)
Pt-N2	2.055 (6)		
N1-Pt-N2	176.6 (2)	N2-Pt-N3	91.4 (3)
N1-Pt-N3	90.5 (3)	N2-Pt-O2′	88.5 (2)
N1-Pt-O2′	89.4 (2)	N3-Pt-O2′	176.3 (2)
Ligand Geometry			
N1-C2	1.347 (8)	C4-C5	1.369 (13)
C2-O2	1.302 (10)	C5-C6	1.395 (11)
C2-C3	1.423 (9)	C6-N1	1.344 (9)
C3-C4	1.370 (12)	N1-O2	2.336 (7)
Pt-N1-C2	123.0 (5)	C2-C3-C4	119.3 (8)
Pt-N1-C6	116.6 (5)	C3-C4-C5	119.9 (8)
C2-N1-C6	119.9 (6)	C4-C5-C6	119.0 (9)
N1-C2-O2	123.7 (7)	C5-C6-N1	121.8 (8)
N1-C2-C3	120.0 (7)	Pt-O2′-C2′	127.2 (4)
O2-C2-C3	116.2 (6)		
Nitrate Anion			
N4-O41	1.237 (9)	O41-N4-O42	119.9 (8)
N4-O42	1.224 (8)	O41-N4-O43	119.1 (7)
N4-O43	1.247 (10)	O42-N4-O43	121.0 (8)

[a] See footnote *a*, Table II. Primed atoms are related to the unprimed atoms by a 2-fold crystallographic axis. Distances have not been corrected for thermal motion.

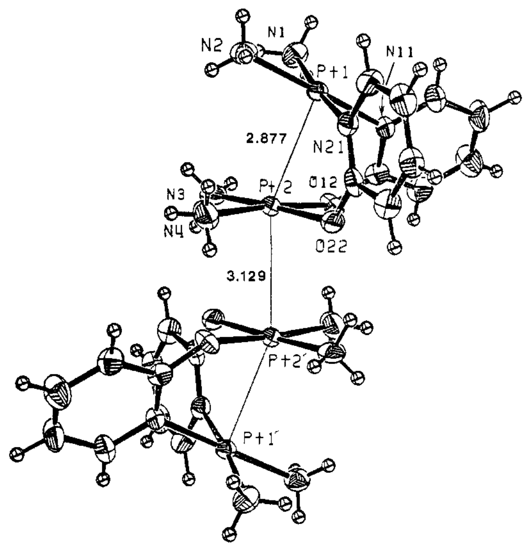

Figure 3. ORTEP illustration of the structure of the head-to-head isomer of the α-pyridonate-bridged cation $[Pt_2(NH_3)_2(C_5H_4NO)_2]^{2+}$ (**2**), showing the 40% probability thermal ellipsoids and the Pt–Pt distances (angstroms). For clarity, the hydrogen atoms are depicted as spheres with *B* set to 1 Å^2. The two halves of the tetranuclear unit are related to each other by a crystallographic inversion center that lies midway between Pt2 and Pt2′. The labels of the hydrogen atoms (not shown) are numbered according to the atom to which they are attached.

that differs from normal four-coordinate Pt(II) stereochemistry is the relatively short 2.898 (1) Å Pt–Pt distance produced in part by the geometric requirements imposed by the bridging α-pyridonate ligands. Bond lengths within the coordination sphere are within the range normally observed in related platinum(II) ammine complexes.[6–15] The longer of the two Pt–NH_3 distances is trans to the heterocyclic nitrogen atom (N1) of the pyridonate ligand, revealing a small structural trans influence.[33] The angles between the adjacent donor atoms within the platinum coordination plane deviate only slightly from 90°. The platinum atom lies 0.057 Å out of the least-squares plane defined by the four ligands, and the direction of the displacement is toward the adjacent Pt atom. The tilt angle between the adjacent platinum coordination planes is 28.8°, and the average torsion angle (or twist) about the Pt–Pt′ vector is 13.0°.

The most significant changes in the geometry of the α-pyridone ring that accompany coordination occur in the bonds and angles at atoms (N1, C2, and O2) adjacent to the Pt binding sites. A comparison of the bond angles of α-pyridone[34] to those in **1** shows a significant decrease in the C6–N1–C2 angle, from 123.5 (3) to 119.9 (6)° (a difference of 5.6σ[35]), and in the O2–C2–C3 angle, from 125.9 (3) to 116.2 (6)° (13.9σ). The removal of the proton, which is found to be on N1 in two crystallographic studies of α-pyridone,[34] from an annular nitrogen in a conjugated ring is generally accompanied by a decrease in the internal angle at the nitrogen and an increase in the adjacent ring angles.[36] This effect

---

(33) Appelton, T. G.; Clark, H. C.; Manzer, L. E. *Coord. Chem. Rev.* **1973**, *10*, 335.

(34) (a) Almlof, J.; Kvick, Å.; Olovsson, I. *Acta Crystallogr., Sect. B* **1971**, *B27*, 1201. (b) Penfold, B. R. *Acta Crystallogr.* **1953**, *6*, 591.

(35) The estimated standard deviation is calculated by using $\sigma = (\sigma_1{}^2 + \sigma_2{}^2)^{1/2}$, where σ_1 and σ_2 are the errors in the bonds or angles being compared.

(36) (a) Singh, C. *Acta Crystallogr.* **1965**, *19*, 861. (b) Lock, C. J. L.; Pilon, P.; Lippert, B. *Ibid.* **1979**, *B35*, 2533.

Table V. Interatomic Distances (Å) and Angles (deg) for $[Pt_2(NH_3)_4(C_5H_4NO)_2]_2(NO_3)_4$ (2)[a]

Coordination Sphere			
Pt1-Pt2	2.8767 (7)	Pt2-Pt2′	3.1294 (9)
Pt1-N1	2.057 (9)	Pt2-N3	2.047 (10)
Pt1-N2	2.063 (9)	Pt2-N4	2.043 (10)
Pt1-N11	2.039 (9)	Pt2-O12	2.035 (8)
Pt1-N21	2.045 (9)	Pt2-O22	2.030 (8)
Pt1-Pt2-Pt2′	158.40 (3)	N3-Pt2-N4	93.6 (5)
N1-Pt1-N2	90.5 (4)	N3-Pt2-O12	86.4 (4)
N1-Pt1-N11	87.9 (4)	N3-Pt2-O22	177.1 (4)
N1-Pt1-N21	174.6 (4)	N4-Pt2-O12	174.9 (4)
N2-Pt1-N11	178.0 (4)	N4-Pt2-O22	87.7 (4)
N2-Pt1-N21	91.3 (4)	O12-Pt2-O22	92.1 (3)
N11-Pt1-N21	90.4 (4)		
Ligand Geometry			
O12-C12	1.294 (15)	O22-C22	1.308 (15)
N11-C12	1.343 (16)	N21-C22	1.328 (18)
C12-C13	1.420 (16)	C22-C23	1.424 (18)
C13-C14	1.37 (2)	C23-C24	1.364 (19)
C14-C15	1.40 (2)	C24-C25	1.37 (2)
C15-C16	1.397 (19)	C25-C26	1.390 (19)
C16-N11	1.352 (16)	C26-N21	1.367 (15)
O12-N11	2.330 (13)	O22-N21	2.300 (13)
Pt1-N11-C12	120.9 (8)	Pt1-N21-C22	124.0 (8)
Pt1-N11-C16	116.8 (8)	Pt1-N21-C26	116.1 (9)
Pt2-O12-C12	124.8 (7)	Pt2-O22-C22	126.1 (8)
C12-N11-C16	121.6 (10)	C22-N21-C26	119.4 (11)
O12-C12-N11	124.1 (10)	O22-C22-N21	121.5 (11)
O12-C12-C13	117.0 (11)	O22-C22-C23	117.9 (12)
N11-C12-C13	118.9 (11)	N21-C22-C23	120.5 (11)
C12-C13-C14	120.6 (13)	C22-C23-C24	119.4 (14)
C13-C14-C15	119.0 (13)	C23-C24-C25	120.0 (13)
C14-C15-C16	119.0 (14)	C24-C25-C26	118.8 (12)
C15-C16-N11	120.7 (13)	C25-C26-N21	121.7 (13)
Anion Geometry			
N7-O72	1.252 (18)	N8-O81	1.20 (2)
N7-O72	1.241 (17)	N8-O82	1.20 (2)
N7-O73	1.232 (16)	N8-O83	1.25 (2)
O71-N7-O72	118.8 (12)	O81-N8-O82	123.0 (16)
O71-N7-O73	121.8 (13)	O81-N8-O83	116.0 (16)
O72-N7-O73	119.0 (13)	O82-N8-O83	120.5 (16)

[a] See footnote *a* to Table III. Distances have not been corrected for thermal motion.

is observed in the geometry of the α-pyridonate ligand in **1**. The decrease in the O2–C2–C3 angle is even larger (9.7 (7)°), and this distortion serves to increase the bite distance of the ligand from 2.269 (5) to 2.336 (7) Å. The increase over 120° in the Pt–N1–C2 (123.0 (5)°) and Pt′–O2–C2 (127.2 (4)°) angles also suggests that the pyridonate ligand has undergone a geometric distortion in order to bridge the ~2.9-Å Pt–Pt′ distance.

The planarity of the α-pyridonate ring is maintained in the head-to-tail dimer, with a root-mean-square deviation of the atoms from the least-squares plane of 0.020 Å. The plane of the pyridonate ring makes an angle of 88.1° with the Pt′ coordination plane, attached to O2, and an angle of 68.4° with the Pt coordination plane, attached to N1. Both Pt atoms lie out of this plane with a deviation of 0.347 Å for Pt and 0.245 Å for Pt′. The angle between the α-pyridonate plane and the O2–Pt′ vector is 6.8°.

The geometry of the nitrate anion is normal (Table IV), and all four atoms define a plane with a root-mean-square deviation of 0.0003 Å. The nitrate anions link the binuclear cations through hydrogen bonds between N2 (N2–O43, 3.04 (1) Å) and N3′ (N3′–O41, 3.00 (1) Å). The N2-ammine ligand is also hydrogen bonded to the pyridonate oxygen atom (O2′) of an adjacent cation (N2–O2′ = 3.00 (1) Å) and to the water molecule of hydration (N2–O1 = 2.99 (1) Å). The water of hydration has two additional hydrogen-bond contacts: to O43 of one nitrate (O1–O43 = 2.75 (2) Å) and to O42′ of another (O1–O42′ = 2.93 (1) Å). Additional hydrogen-bond information (distances and angles) is presented as supplementary material in Table S5.

$[Pt_2(NH_3)_4(C_5H_4NO)_2]_2(NO_3)_4$ (2), Head-to-Head Dimer. As shown in Figure 4, the head-to-head dimer associates in the crystal lattice through hydrogen bonds to a second identical dimeric unit. The two halves of the resulting tetranuclear chain are related to each other through a crystallographic inversion center that lies at the center of the Pt2–Pt2′ vector. The intracation Pt1–Pt2 distance of 2.877 (1) Å is 0.252 (1) Å shorter than the intercation Pt2–Pt2′ distance and is also slightly shorter (0.021 (1) Å) than the corresponding distance in the head-to-tail dimer **1**. The angle between the Pt1–Pt2 and Pt2–Pt2′ vectors in the four-atom chain is 158.40 (3)°. The geometry of the ligands in the Pt coordination planes is normal, with Pt–NH_3 distances of 2.043 (10)–2.063 (9) Å and Pt–N (ring) distances of 2.039 (9) and 2.045 (9) Å. The Pt–O distances are equivalent and do not differ from that found in **1**. Both platinum coordination spheres are planar, with a four-atom root-mean-square deviation of 0.052 Å for the Pt1 plane and 0.034 Å for the Pt2 plane. As observed in the head-to-tail dimer **1**, the platinum atoms are slightly displaced out of the plane toward one another (0.035 Å for Pt1 and 0.067 Å for Pt2). The tilt angle between the two platinum coordination planes is 30.0°, and the average torsion angle about the Pt1–Pt2 vector is 20.3°; both of these values are larger than observed for **1**.

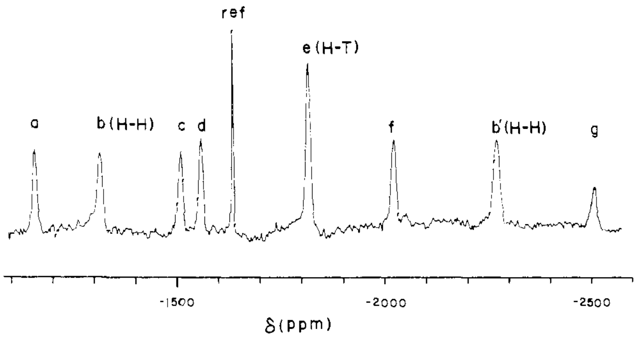

Figure 4. ^{195}Pt NMR spectrum of the products obtained from the reaction of 0.16 M *cis*-$[Pt(NH_3)_2(H_2O)_2](NO_3)_2$ with 1 equiv of α-pyridone (as described in the Experimental Section) after 26 h. The chemical shifts are referenced to $K_2[PtCl_6]$ with negative values indicating a higher field position relative to the reference. The resonances are assigned as follows: (a) hydroxide-bridged dimer $[(NH_3)_2Pt(OH)_2Pt(NH_3)_2]^{2+}$ (**12**), −1153 ppm; (b) head-to-head dimer $[Pt_2(NH_3)_4(C_5H_4NO)_2]^{2+}$ (**2**), −1308 ppm (Pt1); (b′) head-to-head dimer **2**, −2261 ppm (Pt2); (c) hydroxide-bridged trimer $[Pt(NH_3)_2(OH)]_3^{3+}$ (**13**), −1505 ppm; (d) *cis*-$[Pt(NH_3)_2(H_2O)_2]^{2+}$ (**11**), −1556 ppm; (ref) K_2PtCl_4 contained in a coaxial sample tube; (e) head-to-tail dimer $[Pt_2(NH_3)_4(C_5H_4NO)_2]^{2+}$ (**1**), −1810 ppm; (f) α-pyridone monomer *cis*-$[Pt(NH_3)_2(C_5H_4NOH)(H_2O)]^{2+}$ (**3A**), −2015 ppm; (g) bis(α-pyridone) monomer *cis*-$[Pt(NH_3)_2(C_5H_4NOH)_2]^{2+}$ (**14**), −2495 ppm. The pH of the solution was 4.2.

The platinum atoms lie out of the planes of the α-pyridonate ligands, the displacement from the ring 1 plane being 0.396 Å for Pt1 and 0.350 Å for Pt2 and, from the ring 2 plane, 0.583 and 0.491 Å, respectively. The dihedral angle between the platinum coordination planes and the planes of the α-pyridonate ligands are, for ring 1, 82.5° (Pt1 plane) and 67.2° (Pt2 plane) and ring 2, 62.0° (Pt1 plane) and 88.9° (Pt2 plane). The geometry of the α-pyridonate rings in **2** differs from that of α-pyridone in a manner similar to that observed in the case of the head-to-tail isomer **1**.

Hydrogen bonds that connect the two dimeric units across the crystallographic inversion center occur between N3 and O22′ (N3–O22′ = 3.04 (1) Å) and N4 and O12′ (N4–O12′ = 2.95 (1) Å). The tetranuclear units are further linked in the crystal lattice with hydrogen bonds between the ammine ligands and the nitrate anions. The bond lengths and angles in the nitrate anions are normal, and both nitrates are found to be planar, with a four-atom root-mean-square deviation of 0.020 Å for N7-nitrate and 0.018 Å for N8-nitrate. The principal hydrogen bonds to N7-nitrate are between O72 and N2 and O73 and N1′ on an adjacent cation. The N7-nitrate group also connects two adjacent ammines in the same platinum coordination sphere, and as a consequence the plane of the nitrate lies nearly parallel to the Pt1 coordination plane. Additional information on hydrogen bonding (distances and angles) is presented as supplementary material in Table S6.

Table VI. Comparison of Geometric Properties of Related Platinum Complexes

compound	formal Pt oxdn state	Pt-Pt dist, Å	dihedral angle, deg[a] τ	dihedral angle, deg[a] ω	Pt-Pt-Pt angle, deg	ref
$[Pt_2(NH_3)_4(C_5H_4NO)_2](NO_3)_2 \cdot 2H_2O$ (1) α-pyridone, H-T[b] dimer	2.0	2.8981 (5)	28.8	13.0		*c*
$[Pt_2(NH_3)_4(C_5H_4NO)_2]_2(NO_3)_4$ (2) α-pyridone, H-H tetramer	2.0	2.8767 (7) 3.1294 (4)	30.0	20.3	158.40 (3)	*c*
$[Pt_2(NH_3)_4(C_5H_4NO)_2]_2(NO_3)_5 \cdot H_2O$ (4) α-pyridone, H-H tetramer	2.25	2.7745 (4) 2.8770 (9)	27.4	22.8	164.60 (2)	17b
$[Pt_2(NH_3)_4(C_4H_6NO)_2]_2(NO_3)_6 \cdot 3H_2O$ (5) α-pyrrolidone, H-H tetramer	2.5	2.702 (d) 2.709 (d)	18.7	*d*	170.4 (d) 168.8 (d)	37
$[Pt_2(NH_3)_4(C_6H_7N_2O_2)_2](NO_3)_2 \cdot H_2O$ (6) 1-methylthymine, H-T dimer	2.0	2.974 (1)	36.1	13.8		6
$[Pt_2(NH_3)_4(C_5H_5N_2O_2)_2](NO_3)_2 \cdot 3H_2O$ (7) 1-methyluracil, H-T dimer	2.0	2.954 (2)	35.8	19.1		12
$[Pt_2(NH_3)_4(C_5H_6N_3O)_2](NO_3)_2 \cdot 2H_2O$ (8) 1-methylcytosine, H-T dimer	2.0	2.981 (2)	34	16		13
$[Pt_2(NH_3)_4(C_6H_7N_2O_2)_2](NO_3)_2$ (9) 1-methylthymine, H-H dimer	2.0	2.909 (3)	29.5	1.0		14

[a] τ is the tilt angle between adjacent platinum coordination planes in the binuclear unit, and ω is the average torsion angle about the Pt-Pt vector. [b] H-T and H-H are used to indicate that the bridging ligands are oriented in either a head-to-tail or a head-to-head fashion, respectively. [c] This work. [d] Value not reported.

The shortest nonbonded $NH_3 \cdots NH_3$ contacts between ammines that lie in different coordination planes are ~2.9 Å. While this distance is less then the sum of their van der Waals radii, the steric interaction between the ammine ligands is minimized by the twisting (20.3°) of the coordination planes about the Pt1-Pt2 vector.

Structural Comparison with Other Binuclear Complexes of *cis*-Diammineplatinum. The structures of the α-pyridonate bridged complexes of **1** and **2** may be compared with the analogous amidate bridged complexes of 1-methylthymine (**6**)[6] and 1-methyluracil (**7**).[12] A comparison of selected geometric features of these compounds is presented in Table VI. The two *cis*-diammineplatinum(II) units of compound **6** are bridged in a head-to-tail fashion by 1-methylthyminate ligands that are attached to the platinum atom through the O4 exocyclic oxygen and the N3 amidate nitrogen. The geometries of this complex and the head-to-tail isomer of the 1-methyluracilate (N3,O4) bridged complex (**7**) are nearly identical with that of the head-to-tail dimer of α-pyridone (**1**). While the distances and angles within the platinum coordination planes are comparable in all three complexes, the pyrimidinate-bridged complexes have longer (0.076 (1) Å in **6** and 0.056 (1) Å in **7**) Pt-Pt distances. The parameter that shows the largest difference is the tilt angle (τ) between adjacent platinum coordination planes. Since all three compounds have equivalent ligand bite distances, the ~7° increase in τ results from the lengthening of the Pt-Pt distance without relaxing the twist angle (ω) about the Pt-Pt vector.

The structure of **1** can also be compared to the structure of the head-to-tail dimer of 1-methylcytosine, $[(NH_3)_2Pt(C_5H_6N_3O)_2Pt(NH_3)_2](NO_3)_2 \cdot 2H_2O$ (**8**).[13] Although the 1-methylcytosinate ligand in **8** bridges the platinum atoms in an unusual fashion, through N3 and the deprotonated exocyclic amine 4-NH_2, the geometry of this complex is very similar to that of compound **1**. As with the other pyrimidinate-bridged complexes **6** and **7**, the Pt-Pt distance and the interplanar tilt angles (τ) in the cytosinate complex are both larger than in **1** (see Table VI).

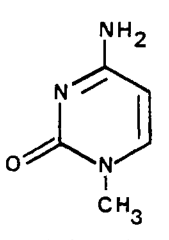

1 methylcytosine

Only a limited structural comparison can be made between the head-to-head isomer of the α-pyridonate dimer **2** and analogous pyrimidinate complexes since only one such structure is known. A brief report on the structure of the head-to-head complex of 1-methylthyminate (**9**, Table VI) was presented.[14] This complex, which contains bridging 1-methylthyminate ligands bound to platinum through N3 and O4, has a geometry that is similar to that of **2**, but it does not form the closely associated hydrogen-bonded pair that is found in the structure of **2**. Rather, the closest intermolecular Pt-Pt distance is 5.615 (3) Å, a value typical of that found in the head-to-tail complexes. The intramolecular Pt-Pt distance in the head-to-head complex **9** is 0.065 (3) Å shorter than the corresponding distance in the head-to-tail isomer **6**. The head-to-head isomer of the α-pyridonate bridged complex also has the shorter Pt-Pt distance of the two isomeric forms. While the head-to-head complexes **2** and **9** have equivalent tilt angles (τ) between the platinum coordination planes, the twist angles (ω) of these planes about the Pt-Pt vector are very different. The platinum coordination planes in **9** are nearly eclipsed ($\omega \sim 1°$). The significance of this unique geometry cannot be assessed until the full details of this structure are presented.

The structure of the head-to-head α-pyridonate dimer **2** bears a striking resemblance to the structure of *cis*-diammineplatinum α-pyridone blue (PPB), **4**. Both complexes are composed of two dimeric units that are related to each other by a crystallographic inversion center that lies at the center of the intermolecular Pt2-Pt2′ vector. The most significant structural differences between the two complexes result from the decrease in the inter- and intracation platinum-platinum distances that occurs because of partial metal-metal bonding in PPB. The removal of one electron from the tetranuclear platinum(II) complex **2** results in a 0.102 (1) Å decrease in the Pt1-Pt2 distance and a 0.252 (1) Å decrease in the Pt2-Pt2′ distance. The shortening of the Pt-Pt distances within the chain is accompanied by an increase in the Pt1-Pt2-Pt2′ angle, from 158.40 (3)° in the platinum(II) complex **2** to 164.60 (2)° in the mixed-valent complex **4**. The dihedral angles between the platinum coordination planes and the planes of the α-pyridonate rings are ~5° larger in the case of ring 2 in **2** (ring 2-Pt1 plane = 91.1°, ring 2-Pt2 plane = 67.2°) while the ring 1 angles are equivalent to those found in PPB.[17] The dihedral angle between the platinum coordination planes (τ) decreases by 2.6°, and the average twist angle about the Pt-Pt vector (ω) increases by 2.8° as the Pt atoms move closer together.

The effect of increasing the platinum chain angle (Pt1-Pt2-Pt2′) and decreasing the interplanar tilt angle (τ) with a shortening of the platinum-platinum distances is further demonstrated in the structure of the *cis*-diammineplatinum complex of α-pyrrolidone (see Figure 1). The α-pyrrolidone complex, $[(NH_3)_2Pt(C_4H_6NO)_2Pt(NH_3)_2]_2(NO_3)_6 \cdot 3H_2O$ (**5**),[37] contains a tetranuclear chain of platinum atoms in an average oxidation state of +2.5.

---

[37] Matsumoto, K.; Fuwa, K. *J. Am. Chem. Soc.* **1982**, *104*, 897.

Table VII. ^{195}Pt NMR Chemical Shifts[a] of *cis*-Diammineplatinum(II) Complexes

complex	chemical shift, ppm[b]	complex	chemical shift, ppm[b]
$[Pt(NH_3)_2(OH)]_2(NO_3)_2$ (**12**)	−1153	$[Pt_2(NH_3)_4(C_5H_4NO)_2](NO_3)_2$ (**1**)	−1810
$[Pt(NH_3)_2(OH)]_3(NO_3)_3$ (**13**)	−1505	*cis*-$[Pt(NH_3)_2(C_5H_4NOH)(H_2O)](NO_3)_2$ (**3A**)[d]	−2015
cis-$[Pt(NH_3)_2(H_2O)_2](NO_3)_2$ (**11**)	−1588[c]	*cis*-$[Pt(NH_3)_2(C_5H_4NOH)_2](NO_3)_2$ (**14**)[d]	−2495
$[Pt_2(NH_3)_4(C_5H_4NO)_2]_2(NO_3)_4$ (**2**)	−1308 −2261		

[a] All chemical shifts are reported relative to K_2PtCl_6; further details are supplied in the Experimental Section. [b] Except where noted, measurements were made at pH 4.2. [c] pH 2.0. [d] At pH 4.2 this species is partially deprotonated.

It is composed of two dimeric units of *cis*-diammineplatinum that are bridged by α-pyrrolidonate ligands in a head-to-head arrangement. While the α-pyrrolidone complex **5** is similar in structure to α-pyridone blue **4** (Table VI), the Pt–Pt distances are on the average 0.12 Å shorter in **5**. The decrease in the Pt–Pt distance is expected since the metal–metal bond order should increase relative to that of PPB with the removal of an additional electron from the tetranuclear platinum chain. While the details of this structure have not been presented in full, the preliminary results show an increase in the Pt–Pt–Pt chain angle angle of ~5° and a decrease in the interplanar tilt angle (τ) of 8.7°. A similar interplanar tilt angle of 20.2° is also found in the structure of the Pt(III) head-to-head α-pyridonate dimer, $[(NO_3)(NH_3)_2Pt(C_5H_4NO)_2Pt(NH_3)_2(H_2O)](NO_3)_3 \cdot 2H_2O$ (**10**),[38] which is obtained by oxidation of PPB with nitric acid. The Pt–Pt distance in this complex is 2.5401 (5) Å, or 0.167 Å shorter than the average Pt–Pt distance in the α-pyrrolidone complex (**5**). This shortening is expected since the Pt(III) dimer contains a Pt–Pt single bond.[38]

One feature that is common to both PPB and the partially oxidized α-pyrrolidone complex, but is lacking in the Pt(II) head-to-head dimer **2**, is the presence of weakly bound nitrate ligands in the axial sites of the platinum atoms in the exterior coordination planes (see Figure 1). While this association is weak in PPB ($Pt \cdots ONO_2$ distance = 3.321 (9) Å), the interaction becomes pronounced as the platinum chain is more highly oxidized. The axial sites in the Pt(III) head-to-head dimer **10** are occupied by NO_3^- and H_2O at distances that are only slightly longer (2.11–2.18 Å) than found in normal Pt–ligand covalent bonds.[38] Axial ligand coordination appears to be a general feature of binuclear Pt(III) complexes. For example, oxidation of the Pt(II) head-to-tail dimer of α-pyridone (**1**) with nitric acid produces the Pt(III) head-to-tail dimer $[(NO_3)(NH_3)_2Pt(C_5H_4NO)_2Pt(NH_3)_2(NO_3)](NO_3)_2 \cdot {}^1/_2H_2O$, which contains a Pt–Pt single bond (Pt–Pt distance, 2.5468 (8) Å) and nitrate ligands bound in the axial sites ($Pt–ONO_2$ = 2.17 Å).[39] Other examples of this property are found in the structures of $K_2[Pt_2(SO_4)_4(H_2O)_2]$,[40] $Na_2[Pt_2(HPO_4)_4(H_2O)_2]$,[41] $K_2[Pt_2(SO_4)_4(OS(CH_3)_2)_2] \cdot 4H_2O$,[42] and $K_4[Pt_2(H_2P_2O_5)_4Cl_2] \cdot 2H_2O$.[43]

Solution Chemistry of *cis*-Diammineplatinum(II) Complexes with α-Pyridone: ^{195}Pt NMR Spectroscopic Studies. The reactions that produce the head-to-tail and head-to-head platinum(II) dimers of α-pyridone were examined by using natural abundance ^{195}Pt NMR spectroscopy. This technique is a convenient method for monitoring the progress of the reactions; good quality spectra were obtained within 10–15 min on 10-mL samples that were ~0.1 M in platinum. The large ^{195}Pt chemical shift range (~15 000 ppm) and the predictable nature of the chemical shifts upon ligand substitution[44] provide an excellent means for product identification in the aqueous solution reactions of *cis*-diammineplatinum(II) complexes.[45]

The reactions of *cis*-$[Pt(NH_3)_2(H_2O)_2](NO_3)_2$ (**11**) in water are quite important determinants in its chemistry with α-pyridone, which ultimately leads to the *cis*-diammineplatinum α-pyridone blue (PPB). Recently a number of reports have appeared on the pH dependent chemical behavior of *cis*-$[Pt(NH_3)_2(H_2O)_2](NO_3)_2$ in aqueous media.[23,24,45,46] The diaquo complex *cis*-$[Pt(NH_3)_2(H_2O)_2]^{2+}$ is stable at low pH (≤2) but undergoes a series of condensation reactions following removal of acidic protons of the coordinated water molecules (pK_1 = 5.6, pK_2 = 7.3)[47] with base. When concentrated solutions of the complex are titrated with 1 equiv of base, the major products that form are the hydroxide-bridged dimer $[(NH_3)_2Pt(OH)_2Pt(NH_3)_2](NO_3)_2$ (**12**),[24] the hydroxide-bridged trimer $[(NH_3)_2Pt(OH)]_3(NO_3)_3$ (**13**),[46] and a distribution of monomeric hydroxyaquo complexes (*cis*-$[Pt(NH_3)_2XY]^{n+}$, where X, Y = OH or H_2O). The oligomerization reactions of *cis*-$[Pt(NH_3)_2(H_2O)_2]^{2+}$ have been examined briefly in several ^{195}Pt NMR studies,[45] and a number of the products of these reactions have been isolated and fully characterized by X-ray diffraction methods.[23,24,46]

The ^{195}Pt chemical shifts of *cis*-diammineplatinum(II) complexes are very sensitive to ligand substitution. A chemical shift range of over 1300 ppm is found in the platinum(II) complexes of the form *cis*-$[Pt(NH_3)_2L_2]^{n+}$, where the ligand L is either a neutral or anionic nitrogen or oxygen donor. The values of the chemical shifts are correlated in a nearly linear fashion with the nature of the donor ligands L. In general, the more electronegative oxygen donor (O_d) produces a chemical shift that is downfield relative to a nitrogen donor (N_d), and therefore the chemical shifts of the complexes *cis*-$[Pt(NH_3)_2L_2]$ are found to increase in the order *cis*-$Pt(NH_3)_2(N_d)_2$ < *cis*-$Pt(NH_3)_2(N_d)(O_d)$ < *cis*-$Pt(NH_3)_2(O_d)_2$. While there are a number of other important factors that influence the chemical shift,[44] this order holds for the complexes that are relevant to the present investigation (vide infra). The measured chemical shifts for the hydrolysis products of *cis*-$[Pt(NH_3)_2(H_2O)_2](NO_3)_2$ in the experiments described below are in good agreement with the values previously reported.[45]

The reaction of *cis*-$[Pt(NH_3)_2(H_2O)_2](NO_3)_2$ with 1 equiv of α-pyridone at an initial pH of 6 for 24 h at 40 °C produces deep green solutions that, when adjusted to pH 1 with nitric acid, provide crystals of both the platinum(II) head-to-tail dimer **1** and platinum α-pyridone blue **4** (see Experimental Section for details). Crystals of the platinum(II) head-to-head dimer **2** are also obtained from this reaction when the pH is not lowered with nitric acid. The products that form during the reactions that occur prior to the addition of nitric acid have been identified by using ^{195}Pt NMR spectroscopy (see Table VII and Figure 4). During the initial stage of the reaction, ~20 min after the pH is adjusted to 6, ^{195}Pt NMR spectra show the major components in solution to be, in order of decreasing concentration, the hydroxide-bridged dimer (**12**), the monohydroxo monomer *cis*-$[Pt(NH_3)_2(OH)(H_2O)]^{2+}$, the hydroxide-bridged trimer (**13**) and a small signal (~8% of the total Pt) at −2043 ppm. The peak at −2043

---

[38] Hollis, L. S.; Lippard, S. J. *J. Am. Chem. Soc.* **1981**, *103*, 6761.

[39] Hollis, L. S.; Lippard, S. J. *Inorg. Chem.* **1982**, *21*, 2116.

[40] Muraveiskaya, G. S.; Kukina, G. A.; Orlova, V. S.; Evstaf'eva, O. N.; Porai-Koshits, M. A. *Dokl. Akad. Nauk SSSR* **1976**, *226*, 596.

[41] Cotton, F. A.; Falvello, L. R.; Han, S. *Inorg. Chem.* **1982**, *21*, 1709.

[42] Cotton, F. A.; Falvello, L. R.; Han, S. *Inorg. Chem.* **1982**, *21*, 2889.

[43] Che, C.-M.; Schaefer, W. P.; Gray, H. B.; Dickson, M. K.; Stein, P. B.; Roundhill, D. M. *J. Am. Chem. Soc.* **1982**, *104*, 4253.

[44] (a) Kidd, G.; Goodfellow, R. J. In "NMR and the Periodic Table"; Harris, R. K., Mann, B. E., Eds.; Academic Press: London, 1978; Chapter 8. (b) Kerrison, S. J. S.; Sadler, P. J. *J. Magn. Reson.* **1978**, *31*, 321. (c) Pregosin, P. S. *Coord. Chem. Rev.* **1982**, *44*, 247.

[45] (a) Rosenberg, B. *Biochemie* **1978**, *60*, 859. (b) Boreham, C. J.; Broomhead, J. A.; Fairlie, D. P. *Aust. J. Chem.* **1981**, *34*, 659. (c) Kerrison, S. J. S.; Sadler, P. J. *J. Chem. Soc., Chem. Commun.* **1981**, 61. (d) O'-Halloran, T. V.; Lippard, S. J., to be submitted for publication. (e) Chikuma, M.; Pollock, R. J. *J. Magn. Res.* **1982**, *47*, 324.

[46] Faggiani, R.; Lippert, B.; Lock, C. J. L.; Rosenberg, B. *Inorg. Chem.* **1977**, *16*, 1192.

[47] (a) Jensen, K. A. *Z. Anorg. Chem.* **1939**, *242*, 87. (b) Perumareddi, J. R.; Adamson, A. W. *J. Phys. Chem.* **1968**, *72*, 414.

ppm corresponds to the chemical shift of the mono-α-pyridone complex *cis*-$[Pt(NH_3)_2(C_5H_4NOH)(H_2O)]^{2+}$ (**3A**), which can also be prepared from the reaction of *cis*-$[Pt(NH_3)_2(C_5H_4NO)Cl]Cl$ (**3**) with $AgNO_3$ as described in the Experimental Section. As with other platinum complexes that have titratable protons, the chemical shift of compound **3A** changes by as much as 30 ppm as a function of pH.[45d] This change is the result of deprotonation of the coordinated water molecule and the hydroxyl group on the pyridine ring, the pK_a values of which remain to be determined. After an additional 12 h at 40 °C, a number of new resonances are found in the NMR spectrum of the product, each of which has an intensity that remains small (<5%) with respect to those of the hydroxide-bridged dimer and trimer. The new peaks correspond to the head-to-tail dimer **1**, the head-to-head dimer **2**, and the bis(α-pyridone) complex *cis*-$[Pt(NH_3)_2(C_5H_4NOH)_2]^{2+}$ (**14**).[21] At this point in the reaction the major component of the α-pyridone-containing products continues to be the mono-α-pyridone complex *cis*-$[Pt(NH_3)_2(C_5H_4NOH)(H_2O)]^{2+}$ (**3A**).

The spectrum of the sample, taken after 26 h at 40 °C, is shown in Figure 4. At this stage in the reaction, the two major components are the head-to-tail dimer **1** (peak e) and the head-to-head dimer **2** (peaks b and b′). The two signals in the head-to-head dimer result from the nonequivalent platinum centers: Pt1 is bound to four nitrogen donors (peak b′), and Pt2 is bound to two oxygen and two nitrogen donors (peak b). From the intensity of the signals, both isomers are estimated to be present in nearly equal amounts. This observation is consistent with the observed yields for compounds **1** and **4** isolated by using the procedure for preparing the platinum α-pyridone blue. Four other species are present in smaller but nearly equivalent amounts. These four products are the hydroxide-bridged dimer **12** (peak a), the hydroxide-bridged trimer **13** (peak c), the diaquo complex **11** (peak d), and the mono-α-pyridone complex **3A** (peak f). The smallest component of the product mixture (peak g) is the bis(α-pyridone) complex **14**.

The results of this experiment clearly demonstrate that, at the point of acidification in the preparation of platinum α-pyridone blue, the head-to-head platinum(II) dimer is a major component in solution. When the pH of the solution is lowered from 4.2 to 1.0 with nitric acid, the solution rapidly changes from green to deep blue as the head-to-head platinum(II) complex is oxidized to the mixed-valent complex **4**. One important feature of this chemistry that could prove useful in the study of the platinum-pyrimidine blue system is that the degree of oxidation can be controlled by regulating the pH. It may also be possible to stabilize the products in the pyrimidine system toward oxidation through control of pH. While the mechanism of oxidation remains to be determined, electrochemical studies on the α-pyridonate complexes[38] suggest that electron-exchange reactions between the head-to-head Pt(II) and Pt(III) dimers may be involved in the formation of the partially oxidized tetramer **4**.

An examination of the chemical shift values of the products that contain α-pyridone shows the binuclear complexes to have resonances that are shifted downfield relative to the corresponding mononuclear analogues. Thus, although the chemical environment of the platinum atoms in the head-to-tail dimer **1** is similar to that of the mononuclear α-pyridone complex *cis*-$[Pt(NH_3)_2(C_5H_4NOH)(H_2O)]^{2+}$ with respect to the primary coordination sphere, the average chemical shift difference between the two complexes is ~220 ppm. A similar difference occurs between the chemical shifts of the nitrogen-bound platinum (Pt1) of the head-to-head dimer **2** and the platinum in the bis(α-pyridone) monomer *cis*-$[Pt(NH_3)_2(C_5H_4NOH)_2]^{2+}$ and also between the oxygen-bound platinum (Pt2) of the head-to-head dimer and that of the diaquo complex *cis*-$[Pt(NH_3)_2(H_2O)_2]^{2+}$. Since the Pt chemical shifts of these mononuclear complexes change by only 30–50 ppm with pH, it is unlikely that differences in charge are responsible for a downfield shift of this magnitude. Although the exact origin of the chemical shift difference has not been established in this study, the effect presumably results from an interaction between the adjacent metal centers. The metal–metal interaction in binuclear α-pyridonate-bridged complexes of platinum(II) can be considered significant, judging from the Pt–Pt distances. These distances are comparable to those in the partially oxidized one-dimensional complexes such as $K_{1.75}[Pt(CN)_4]\cdot 1.5H_2O$[48] (Pt–Pt = 2.967 Å) and $K_2[Pt(CN)_4]Br_{0.3}\cdot 3H_2O$[49] (Pt–Pt = 2.890 Å), which contain delocalized, partial metal–metal bonds.[50] A downfield shift in the ^{195}Pt NMR signal of the partially oxidized $K[Pt(CN)_4]Br_{0.3}(H_2O)_x$ species relative to the Pt(II) complex $K_2[Pt(CN)_4]$ has been attributed to the Knight shift,[51] which results from the hyperfine interaction between the ^{195}Pt nucleus and the conduction electrons. While the metal–metal interaction in the binuclear complexes is not a highly delocalized one, a net bonding situation can be obtained from a stabilization of the occupied $\sigma(5d_{z^2} + 5d_{z^2})$ and $\sigma^*(5d_{z^2} - 5d_{z^2})$ molecular orbitals through orbital mixing with the symmetry-equivalent set of unoccupied metal-based $\sigma(6p_z + 6p_z)$ and $\sigma^*(6p_z - 6p_z)$ molecular orbitals.[52] The quantitative dependence of the ^{195}Pt chemical shift upon the strength of the metal–metal interaction in binuclear platinum(II) complexes is a subject for further investigation.

A second method of preparing the α-pyridonate bridged dimers **1** and **2** is from the reaction between α-pyridone and the hydroxide-bridged dimer $[(NH_3)_2Pt(OH)_2Pt(NH_3)_2](NO_3)_2$ at pH 10. This reaction also produces a variety of products similar to that found in the reaction with *cis*-$[Pt(NH_3)_2(H_2O)_2]^{2+}$. The major difference between the two methods is a kinetic one. A similar product distribution is evident from the ^{195}Pt spectrum only after the reaction has occurred for more than 5 days. A decrease in the reaction rate between the ethylenediamine complex $[Pt(en)(H_2O)_2]^{2+}$ and uracil in an alkaline medium (pH ~9) has also been observed.[15] The decrease in rate under basic conditions is presumably due to the more inert behavior of the hydroxide ligand in platinum(II) substitution reactions, a feature that is common to platinum(II) complexes.[53]

Conclusions

The platinum(II) complexes obtained in the reactions of *cis*-$[Pt(NH_3)_2(H_2O)_2]^{2+}$ with α-pyridone are closely related to the products that are obtained in analogous reactions of free and substituted pyrimidines. The structures of two isomeric forms of α-pyridonate-bridged binuclear complexes of *cis*-diammineplatinum(II) have been determined by using X-ray crystallographic and ^{195}Pt NMR spectroscopic techniques. The structure of the head-to-tail platinum(II) dimer of α-pyridone is similar to the structures of the binuclear complexes of *cis*-diammineplatinum(II) that contain bridging 1-methylthyminate or 1-methyluracilate ligands. The molecular geometry of the head-to-head platinum(II) tetramer $[Pt_2(NH_3)_4(C_5H_4NO)_2]_2^{4+}$ corresponds closely to that of the platinum α-pyridone blue cation $[Pt_2(NH_3)_4(C_5H_4NO)_2]_2^{5+}$, with the exception of longer (0.1–0.2 Å) Pt–Pt distances owing to the differences in the metal–metal bond order for the two compounds. Both head-to-head and head-to-tail dimers have been found, from ^{195}Pt NMR studies, to form in equal proportions in the reaction that leads to the formation of PPB. Addition of nitric acid (pH 1) to these solutions converts the head-to-head platinum(II) complex to the platinum blue analogue while leaving the head-to-tail complex in the platinum(II) oxidation state. The importance of pH in controlling oxidation state in the α-pyridonate complexes of platinum has been established and could possibly

---

(48) Reis, A. H., Jr.; Peterson, S. W.; Washecheck, D. M.; Miller, J. S. *Inorg. Chem.* **1976**, *15*, 2455.

(49) Williams, J. W.; Peterson, J. L.; Gerdes, H. M.; Peterson, S. W. *Phys. Rev. Lett.* **1974**, *33*, 1079.

(50) For a review of one-dimensional inorganic complexes see: Miller, J. S.; Epstein, A. J. *Prog. Inorg. Chem.* **1976**, *20*, 1.

(51) (a) Rupp, H. H. *Z. Naturforsch. A* **1971**, *26*, 1937. (b) Niedoba, H.; Launois, H.; Brinkman, D.; Brugger, R.; Zeller, H. R. *Phys. Status Solidi B* **1973**, *58*, 309. (c) Keller, H. J.; Rupp, H. H. *Z. Naturforsch. A* **1971**, *26*, 2066.

(52) (a) Mann, K. R.; Gordon, J. G.; Gray, H. B. *J. Am. Chem. Soc.* **1975**, *97*, 3553. (b) Mann, K. R.; Lewis, N. S.; Williams, R. M.; Gray, H. B. *Inorg. Chem.* **1978**, *17*, 828. (c) Messmer, R. P.; Interrante, L. V. *Chem. Phys. Lett.* **1974**, *26*, 225.

(53) For a review see: Howe-Grant, M. E.; Lippard, S. J. *Metal Ions Biol. Syst.* **1980**, *11*, 63.

be used in the synthesis of related amidate-bridged complexes. This chemistry provides a foundation for understanding the more complex chemistry that leads to the platinum pyrimidine blues and further illustrates the diverse nature of the reactions that occur between *cis*-diammineplatinum and cyclic amidate ligands.

Acknowledgment. This work was supported by National Institutes of Health Research Grant CA 15826. We also thank Thomas V. O'Halloran for experimental assistance with the ^{195}Pt NMR spectral measurements and Engelhard Industries for a loan of $K_2[PtCl_4]$ used to make all platinum complexes described.

Registry No. **1**, 85336-85-2; **2**, 76761-63-2; **3**, 85336-86-3; **3A**, 85336-88-5; **11**, 52241-26-2; *cis*-$[Pt(NH_3)_2(NO_3)_2]$, 41575-87-5; $[Pt_2(NH_3)_4(OH)_2](NO_3)_2$, 62048-58-2; *cis*-$[Pt(NH_3)_2Cl_2]$, 15663-27-1; ^{195}Pt, 14191-88-9.

Supplementary Material Available: Atomic positional and thermal parameters, hydrogen bond distances, and observed and calculated structure factors for **1** and **2** (22 pages). Ordering information is given on any current masthead page.

Concerning the Structure and Stability of a Copper(I) Alkoxy Carbonyl

Rolf L. Geerts, John C. Huffman, Kirsten Folting, Timothy H. Lemmen, and Kenneth G. Caulton*

Contribution from the Department of Chemistry and Molecular Structure Center, Indiana University, Bloomington, Indiana 47405. *Received November 8, 1982*

Abstract: The product of carbonylation (Saegusa, 1974) of planar $(CuO\text{-}t\text{-}Bu)_4$ is shown to retain its state of aggregation: the product is $[CuCO(O\text{-}t\text{-}Bu)]_4$, which is shown by X-ray crystallography to have a Cu_4O_4 core of cubane form. Copper is four-coordinate and coordinatively saturated, exhibiting a trigonally distorted tetrahedral geometry. Evidence from spectroscopic measurements and reactivity studies indicates that the cubane tetramer dissolves unchanged in benzene. The ^{13}C resonance of the coordinated carbonyl, 173 ppm, is upfield of free CO and exhibits coupling to the quadrupolar copper nucleus. The ^{63}Cu NMR spectrum of $[Cu(^{13}CO)O\text{-}t\text{-}Bu]_4$ shows a doublet, indicating that the tetramer dissolves to give a single species and that the CO ligand undergoes neither dissociation nor intramolecular scrambling. An argument is presented to account for the high resistance of $[CuCO(O\text{-}t\text{-}Bu)]_4$ toward decarbonylation. The argument naturally accounts for the comparable stability observed for two other Cu(I) carbonyls. X-ray crystallographic parameters: $a = b = 10.431$ (3) Å, $c = 32.024$ (12) Å, and $\gamma = 120°$ with $Z = 4$ in space group $P\bar{3}c1$ (No. 165).

The carbonyl chemistry of Cu(I) is unusual in having achieved perhaps more commercial than fundamental importance. Cuprous carbonyls are responsible for scavenging CO from gas streams,[1,2] and they are probably implicated in the low-pressure conversion of synthesis gas to methanol.[3-5] Cuprous carbonyls are characterized by two properties;[6] their instability toward decarbonylation and their relatively high $C\equiv O$ stretching frequency. In recent years, Floriani's group has been influential in establishing the stoichiometry and the spectroscopic and structural features of cuprous carbonyls.[7] His results, employing halo and, mainly, amine ligands, have generally reaffirmed the characteristics of Cu(I) carbonyls stated above. Employing benzoate as a bridging ligand, he has produced a remarkable μ-bridging carbonyl.[7]

We have been attempting to establish, for soluble copper hydrides[8] and copper carbonyls, reaction patterns of possible relevance to the heterogeneous low-pressure methanol synthesis. In this regard, the earlier report of Saegusa et al.[9] that $(CuO\text{-}t\text{-}Bu)_4$ is carbonylated to the first thermally stable (i.e., sublimes in vacuum at 66 °C) copper carbonyl, "$CuCO(O\text{-}t\text{-}Bu)$," was intriguing. The degree of aggregation of this species is unknown, as is its structure. We were also interested in a possible structural basis for the thermal stability[10] of this carbonyl, particularly since this is the only known carbonyl with an exclusively oxygen-based coligand environment. Finally, such structural information may be revealing with respect to the heterogeneous methanol catalyst, since it originates from the oxides of copper and zinc.

Experimental Section

All operations were performed under an N_2 atmosphere by using standard Schlenk techniques for air- and moisture-sensitive materials. Hexanes and tetrahydrofuran were distilled under N_2 prior to use from solutions of the sodium benzophenone ketyl. $(CuO\text{-}t\text{-}Bu)_4$ was prepared as previously described.[9] IR spectra were recorded either in a standard solution cell (0.1-mm path length, room temperature) or in a locally fabricated low-temperature (−78 °C) cell.[12] NMR spectra were recorded either at 220 MHz (^1H) or at 90.8 MHz (^{13}C) in benzene-d_6 and referenced to internal Me_4Si. Enriched ^{13}CO was purchased from Mound Laboratory.

---

(1) Walker, D. G. *Chemtech.* **1975**, *5*, 308.

(2) "Kirk-Othmer Encyclopedia of Chemical Technology"; Wiley: New York, 1978; p 788.

(3) Natta, G. *Catalysis* **1955**, *3*, 349. P. H. Emmett, ed.

(4) Kung, H. L. *Catal. Rev.* **1980**, *22*, 235.

(5) Herman, R. G.; Klier, K.; Simmons, G. W.; Finn, B. P.; Bulko, J. B.; Kobylinski, T. P. *J. Catal.* **1979**, *56*, 407.

(6) Bruce, M. I. *J. Organomet. Chem.* **1972**, *44*, 209.

(7) Pasquali, M.; Fluoriani, C.; Venturi, G.; Gaetani-Manfredotti, A.; Chiesi-Villa, A. *J. Am. Chem. Soc.* **1982**, *104*, 4092 and references therein.

(8) Goeden, G. V.; Caulton, K. G. *J. Am. Chem. Soc.* **1981**, *103*, 7354.

(9) Tsuda, T.; Habu, H.; Horiguchi, S.; Saegusa, T. *J. Am. Chem. Soc.* **1974**, *96*, 5930.

(10) We define several operational tests of "stability". At the lower level, many copper carbonyls suffer decarbonylation when N_2 is passed through a solution of the compound. A more stable set of complexes are decarbonylated only when their solution is heated under an inert atmosphere; the COSORB system[1,2] relies on this level of stability. The most stable copper carbonyl survives vacuum sublimation; only $CuCO(O\text{-}t\text{-}Bu)$ passes this test. Such stability is quite possibly kinetic in origin, since one five-coordinate copper carbonyl[11] has a CO binding constant of over 10^4, but it decarbonylates in solution under an N_2 purge.

(11) Gagne, R. R.; Alleson, J. L.; Gall, R. S.; Koval, C. A. *J. Am. Chem. Soc.* **1977**, *99*, 7170.

(12) Lewis, L. N.; Caulton, K. G. *Inorg. Chem.* **1980**, *19*, 1840.

0002-7863/83/1505-3503$01.50/0